ISBN: 978-3-95450-261-5 ISSN: 2673-7000 doi: 10.18429/JACoW-NAPAC2025-WEP047

INVESTIGATING DIRAC SEMIMETAL CADMIUM ARSENIDE AS A POTENTIAL LOW-MTE PHOTOCATHODE

T. W. Idso*, A. Ullattuparambil, M. M. Rizi, S. Karkare, Arizona State University, Tempe, AZ, USA
A. Rice, K. Alberi, National Renewable Energy Laboratory, Golden, CO, USA

Abstract

We report on the quantum efficiency (QE) and mean transverse energy (MTE) of photoemitted electrons from cadmium arsenide (Cd_3As_2), a three-dimensional Dirac semimetal (3D DSM) of interest for photocathode applications due to its unique electronic band structure, characterized by a 3D linear dispersion relation at the Fermi energy. Samples were synthesized at the National Renewable Energy Laboratory (NREL) and transferred under ultra-high vacuum to Arizona State University (ASU) for measurement using a photoemission electron microscope (PEEM). The maximum QE was measured to be $3.37 \cdot 10^{-4}$ at 230 nm, and the minimum MTE was 55.8 meV at 250 nm. These findings represent the first reported QE and MTE measurements of Cd_3As_2 and are an important step in evaluating the viability of 3D DSMs as low-MTE photocathodes. Such photocathodes, constrained to lower MTEs by the electronic band structure, may prove effective in advancing beam brightness in next-generation instruments and techniques.

INTRODUCTION

Minimizing the mean transverse energy (MTE) of photoemitted electrons and maximizing the quantum efficiency (QE) are both essential for the generation of bright electron beams. Existing x-ray free electron lasers (XFELs) and emerging concepts for compact XFELs will directly benefit from higher beam brightness which enables stronger lasing gain, shorter pulse durations, and improved temporal coherence [1–3]. Brighter beams can also alleviate the need for larger accelerator footprints, reducing both operational costs and the complexity of beamline components [4]. Additionally, methods like ultrafast electron diffraction and microscopy (UED/UEM) will benefit from enhanced brightness in terms of higher-contrast imaging and improved temporal resolution [5–8]. Achieving low MTEs and high QEs in photocathodes can thus drive significant advances in the design of next-generation instruments and methods where both performance and scalability are critical considerations. However, finding robust photocathodes that meet these criteria is ongoing.

Three-dimensional Dirac semimetals (3D DSMs) are a novel class of materials which are bulk electronic analogues to graphene (a 2D DSM). 3D DSMs exhibit a distinct electronic structure at the Fermi energy in which the dispersion relation is linear in all three momentum directions around the Dirac point thus resulting in several unique phenomena including massless fermions [9].

* tidso@asu.edu

It has been shown previously that emission from bands with low effective mass can theoretically constrain the transverse momentum of emitted electrons [10, 11]. Likewise, electrons that are photoemitted from near the Dirac point can have exceptionally small transverse energies resulting in MTEs potentially below 5 meV, even at room temperature [2]. Consequently, a robust 3D DSM photocathode is of significant interest for the development of brighter electron beams. Cadmium arsenide (Cd_3As_2), which has attracted significant attention following the experimental observation of its 3D DSM phase via angle-resolved photoemission spectroscopy (ARPES) in 2014, is one candidate for such a photocathode [9, 12, 13]. In this proceeding, we present experimental measurements of QE and MTE from Cd_3As_2, address the experimental dispersion relation at room temperature, and investigate the merits of the interstate transport process used for in-vacuum transfer of the Cd_3As_2 photocathode.

EXPERIMENTAL METHODS

Samples were grown on n-type Si:GaAs[001] substrates with a 4 degree miscut toward (111)A. Following desorption of the surface oxide, a 500 nm Si:GaAs buffer was grown, after which samples were capped and moved to a separate II-VI chamber. A thin ZnTe nucleation layer was then grown after decapping, followed by lattice-matched $Zn_xCd_{1-x}Te$ (approximately 20 and 100 nm thick, respectively). Cd_3As_2 was then grown from a Cd effusion source and an As valved cracker cell as described elsewhere [14]. The growth was performed under As-rich conditions and at a temperature of approximately 115 °C. This layer was grown to a thickness of ∼200 nm before the samples were transferred into an ultra-high vacuum (UHV) "suitcase" with a baseline pressure of 10^{-10} Torr.

The UHV suitcase included an ion pump and power supply which provided continual active pumping throughout the duration of the ∼12-hour interstate transfer process from NREL to ASU. Upon arrival, the suitcase was connected to the UHV transfer line in the Photoemission and Bright Beams Lab (PBBL) [15]. The junction was flushed with an inert gas during the connection procedure to minimize air contamination. A bakeout was then performed overnight to bring the vacuum level in the connecting junction down to the high 10^{-10} Torr range before the vacuum suitcase was opened and the samples were transported into PBBL's UHV transfer line via the magnetically coupled transfer arm installed on the suitcase.

After completing the in-vacuum transfer process, the QE and MTE measurements were performed using a photoemission electron microscope (PEEM) [16]. The pressure in the

ISBN: 978-3-95450-261-5 ISSN: 2673-7000 doi: 10.18429/JACoW-NAPAC2025-WEP047

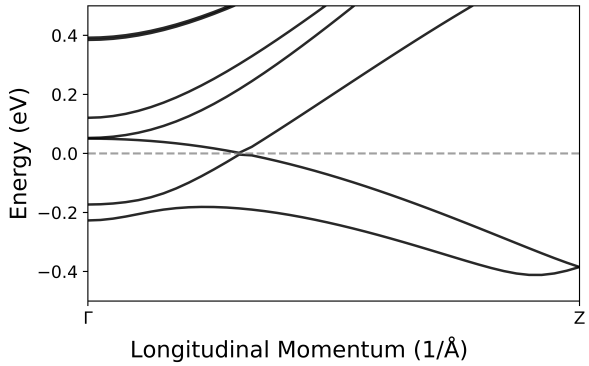

Figure 1: Theoretical band structure of Cd_3As_2 in the longitudinal ($\Gamma - Z$) direction, calculated using VASP. The Dirac point is observed as a linear dispersion at the Fermi energy.

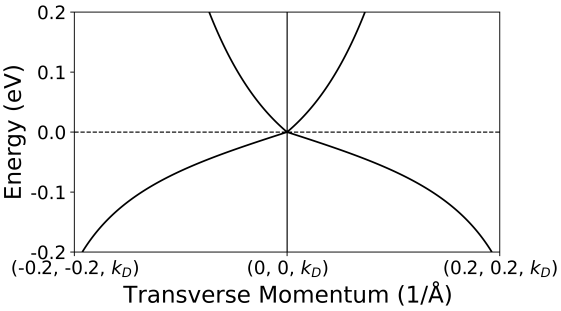

Figure 2: Theoretical band structure of Cd_3As_2 in the transverse directions at the Dirac point, calculated using VASP.

PEEM chamber was in the 10^{-11} Torr range throughout the duration of the measurement process. In total, ~48 hours elapsed between growth and measurement.

All measurements were conducted using a 500 kHz repetition rate, 150 femtosecond pulsed LASER source generated by a Light Conversion Orpheus optical parametric amplifier (OPA) pumped by a Light Conversion Pharos. A more detailed description of the QE and MTE measurement procedure can be found in Ref. [17] along with more information regarding the instrumentation.

The LASER was incident on the (001) surface of the Cd_3As_2 photocathode. This orientation was chosen to align the Dirac point with the longitudinal photoemission direction as the Dirac point is located along the $\Gamma - Z$ high symmetry line (see Fig. 1) [13, 18].

Knowing the location of the Dirac point, we can estimate the MTE of photoemitted electrons by considering the energy dispersion in the transverse momentum directions at that location. Using the relation:

$$E_\perp = \frac{\hbar^2}{2m_e}(k_x^2 + k_y^2),$$

Figure 2 demonstrates that emission close to the Fermi energy can result in transverse energies on the order of 5 meV. This prediction is in agreement with theory and ARPES experimental data as reported by Neupane *et al.* [13].

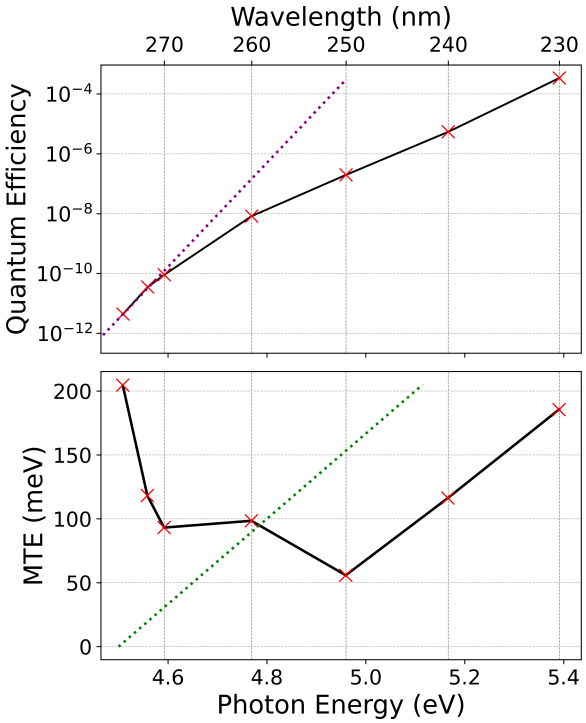

Figure 3: Cd_3As_2 spectral response (top). The QE reaches a peak of $3.37 \cdot 10^{-4}$ at 230 nm. The purple line has a slope of 40 eV^{-1} ($1/k_BT$ at room temperature). The average MTE as a function of photon energy (bottom). The green line shows the Dowell-Schmerge model prediction in which the MTE increases above the work function with a slope of $1/3 \cdot$ Excess Energy. Here, we have used a work function of 4.5 eV as reported in Ref. [22] and in agreement with the spectral response data.

RESULTS AND DISCUSSION

The spectral response in Fig. 3 indicates a maximum quantum efficiency of $3.37 \cdot 10^{-4}$ at a photon wavelength of 230 nm. This value is much lower than state-of-the-art alkali-antimonide photocathodes which can have QEs on the order of 1 % in the visible range [19]. However, it is comparable to generic copper photocathodes which tend to operate with QEs around 10^{-5} to 10^{-4} in the UV range and under optimal conditions [20].

The MTE displays a minimum of 55.8 meV at a photon wavelength of 250 nm. This value is roughly one order of magnitude higher than expected. Thermal effects could be responsible for this behavior and cryogenic techniques will be utilized to reduce these effects in a future study. Additionally, other research has shown that adsorbates and other surface non-uniformities can play a critical role in increasing MTE by the order of magnitude observed here [21].

Previous work by Huang *et al.* reported a work function of 4.5 eV [22]. This is in good agreement with our data as indicated by the spectral response (see the purple dotted line in Fig. 3). However, the Dowell-Schmerge (D-S) model predicts a linear rise in MTE with respect to excess energy for ideal photocathodes [23, 24]. Here we observe

ISBN: 978-3-95450-261-5 ISSN: 2673-7000 doi: 10.18429/JACoW-NAPAC2025-WEP047

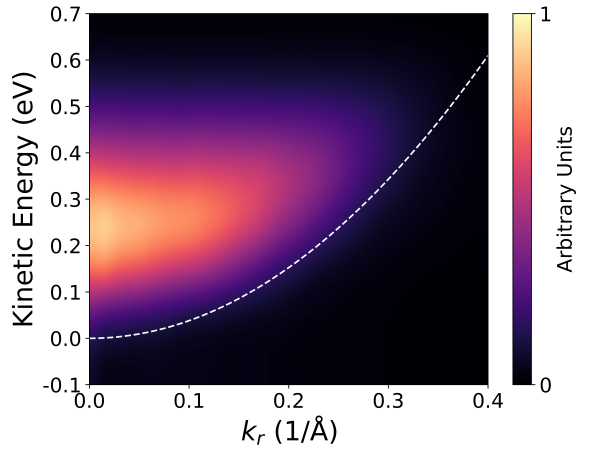

Figure 4: Kinetic energy of photoemitted electrons as a function of radial wavevector for photoemission with 230 nm wavelength photons. The white dashed curve indicates the dispersion of the free electron parabola.

a non-monotonic behavior in the MTE with respect to increasing photon energy, evidenced by the elbow feature at 260 nm. Further evidence of this elbow feature can be seen in the change of slope in the spectral response at that same wavelength.

Pierce *et al.* encountered a similar non-monotonicity in Cs-Te photocathodes [25]. They showed that this behavior can be credibly attributed to a compounded distribution of multiple photoemitting materials or surface orientations where the MTE is given by a weighted sum of the individual MTEs:

$$\mathrm{MTE}(\hbar\omega) = \frac{\sum_i w_i \mathrm{QE}_i(\hbar\omega)\mathrm{MTE}_i(\hbar\omega)}{\sum_i w_i \mathrm{QE}_i(\hbar\omega)}$$

Here, MTE_i and QE_i are the MTE and QE of the i-th material (or surface orientation) in the compound, w_i is the weight of that material (or orientation) within the compound, and $\hbar\omega$ is the incident photon energy.

In our case, the Cd_3As_2 samples were prepared to be atomically well-ordered and single-crystalline. However, it is possible that adsorbate patches could have formed during the extended transfer period and acted as the multiple photoemitting materials described by Pierce *et al.* We estimate a sample exposure of ∼15 L (langmuir) due to the prolonged transfer period. Even with a low sticking coefficient, this exposure could be enough to explain the formation of adsorbate patches in UHV conditions. More data are needed to determine the validity of this theory. It is also possible that this elbow feature could be a property of the material's density of states near the Fermi level in which case it should be easily reproduced in future studies.

We also observe that all emitted electrons occupy a free electron parabola as shown in Fig. 4. However, this occupation is not uniform as would be expected in a D-S scheme [24]. Instead, there is a high intensity region that is maximized around $0.2 - 0.3$ eV at $k_r = 0$ Å^{-1} ($k_r = \sqrt{k_x^2 + k_y^2}$). Similar high intensity regions are seen for every photon wavelength. It is possible that this non-uniformity is a feature related to the anticipated Dirac cone structure, but there is no obvious Dirac cone discerned at any of the photon wavelengths. The lack of a Dirac cone feature may be explained by the temperature broadening of the electron energies due to the sample being analyzed without any cryogenic cooling, in contrast with the existing ARPES literature on Cd_3As_2.

It is also possible that the previously theorized adsorbate monolayer could be resulting in photoemission populating the usual parabolic dispersion, overlapping with and obscuring the Dirac cone structure. In this scenario, it would likely be necessary to maintain vacuum pressures of $\sim 10^{-11}$ Torr or lower for the entire duration of the experiment in order to prevent such monolayer formation.

CONCLUSION

In this proceeding, we have reported on the quantum efficiency and mean transverse energy of cadmium arsenide (Cd_3As_2) photocathodes. Such Dirac semimetal photocathodes are theoretically capable of MTEs lower than 5 meV due to transverse momentum constraints resulting from the unique electronic band structure of these materials. However, the MTEs observed here were an order of magnitude higher than expected, likely due to thermal effects or surface adsorbate patches that formed during the prolonged transfer process.

Future research will focus on implementing a more robust and expedited in-vacuum transfer process along with cryogenic measurements in order for Cd_3As_2 to achieve MTEs low enough to be considered viable for next-generation instruments and techniques. Such improvements may also help resolve the Dirac cone structure which was not directly observed here.

ACKNOWLEDGMENTS

This work was supported by the U.S. National Science Foundation Center for Bright Beams under award No. PHY-1549132 and the Department of Energy (DOE) under Grant No. DE-SC0021092.

This work was also authored, in part, by the National Renewable Energy Laboratory for the U.S. DOE under Contract No. DE-AC36-08GO28308. Funding for the sample growth was provided by the U.S. DOE, Office of Science, Basic Energy Sciences, Division of Materials Sciences and Engineering, Physical Behavior of Materials Program under the Disorder in Topological Semimetals project. The views expressed in the article do not necessarily represent the views of the DOE or the U.S. Government. The U.S. Government retains (and the publisher, by accepting the article for publication, acknowledges that the U.S. Government retains) a nonexclusive, paid-up, irrevocable, worldwide license to publish or reproduce the published form of this work, or allow others to do so, for U.S. Government purposes.

ISBN: 978-3-95450-261-5 ISSN: 2673-7000 doi: 10.18429/JACoW-NAPAC2025-WEP047

REFERENCES

[1] C. Pellegrini, "The history of X-ray free-electron lasers", *Eur. Phys. J. H*, vol. 37, pp. 659–708, 2012. doi:10.1140/epjh/e2012-20064-5

[2] P. Musumeci *et al.*, "Advances in bright electron sources", *Nucl. Instrum. Methods Phys. Res. A*, vol. 907, pp. 209–220, 2018. doi:10.1016/j.nima.2018.03.019

[3] P. Emma *et al.*, "First lasing and operation of an ångstrom-wavelength free-electron laser", *Nat. Photonics*, vol. 4, pp. 641–647, 2010. doi:10.1038/nphoton.2010.176

[4] J. B. Rosenzweig *et al.*, "An ultra-compact x-ray free-electron laser", *New J. Phys.*, vol. 22, p. 093 067, 2020. doi:10.1088/1367-2630/abb16c

[5] D. J. Flannigan and A. H. Zewail, "4D electron microscopy: Principles and applications", *Acc. Chem. Res.*, vol. 45, pp. 1828–1839, 2012. doi:10.1021/ar3001684

[6] B. W. Reed *et al.*, "The evolution of ultrafast electron microscope instrumentation", *Microsc. Microanal.*, vol. 15, pp. 272–281, 2009. doi:10.1017/S1431927609090394

[7] S. P. Weathersby *et al.*, "Mega-electron-volt ultrafast electron diffraction at SLAC National Accelerator Laboratory", *Rev. Sci. Instrum.*, vol. 86, p. 073 702, 2015. doi:10.1063/1.4926994

[8] S. Manz *et al.*, "Mapping atomic motions with ultrabright electrons: Towards fundamental limits in space-time resolution", *Faraday Discuss.*, vol. 177, pp. 467–491, 2015. doi:10.1039/C4FD00204K

[9] Z. K. Liu *et al.*, "A stable three-dimensional topological Dirac semimetal Cd_3As_2", *Nat. Mater.*, vol. 13, pp. 677–681, 2014. doi:10.1038/nmat3990

[10] W. A. Schroeder, T. Li, and B. Rickman, "PbTe(111): DFT analysis and experimental results", the Photocathode Physics for Photoinjectors (P3) Workshop, Newport News, VA, USA, Oct. 2016, Presented at the Photocathode Physics for Photoinjectors (P3) Workshop, Newport News, VA, 17–19 October 2016, 2016.

[11] S. Karkare *et al.*, "Reduction of intrinsic electron emittance from photocathodes using ordered crystalline surfaces", *Phys. Rev. Lett.*, vol. 118, no. 16, p. 164 802, 2017. doi:10.1103/PhysRevLett.118.164802

[12] S. Borisenko, Q. Gibson, D. Evtushinsky, V. Zabolotnyy, B. Büchner, and R. J. Cava, "Experimental realization of a three-dimensional Dirac semimetal", *Phys. Rev. Lett.*, vol. 113, p. 027 603, 2014. doi:10.1103/PhysRevLett.113.027603

[13] M. Neupane *et al.*, "Observation of a three-dimensional topological Dirac semimetal phase in high-mobility Cd_3As_2", *Nat. Commun.*, vol. 5, p. 3786, 2014. doi:10.1038/ncomms4786

[14] A. D. Rice *et al.*, "Epitaxial Dirac semimetal vertical heterostructures for advanced device architectures", *Adv. Funct. Mater.*, vol. 32, no. 21, p. 2 111 470, 2022. doi:10.1002/adfm.202111470

[15] C. Knill, J. Conway, B. Dunham, S. Karkare, H. Padmore, and K. Smolenski, "Design of the ASU photocathode lab", in *Proc. NAPAC'19*, Lansing, MI, USA, pp. 132–135, 2019. doi:10.18429/JACoW-NAPAC2019-MOPLM15

[16] "Focus peem". See https://www.focus-gmbh.com for more information on the FOCUS PEEM., https://www.focus-gmbh.com

[17] A. Kachwala, O. Chubenko, D. Kim, E. I. Simakov, and S. Karkare, "Quantum efficiency, photoemission energy spectra, and mean transverse energy of ultrananocrystalline diamond photocathode", *J. Appl. Phys.*, vol. 132, p. 224 901, 2022. doi:10.1063/5.0130114

[18] M. N. Ali, Q. Gibson, S. Jeon, B. B. Zhou, A. Yazdani, and R. J. Cava, "The crystal and electronic structures of Cd_3As_2, the three-dimensional electronic analogue of graphene", *Inorg. Chem.*, vol. 53, no. 8, pp. 4062–4067, 2014. doi:10.1021/ic403163d

[19] W. G. Stam *et al.*, "Growth of ultra-flat ultra-thin alkali antimonide photocathode films", *APL Mater.*, vol. 12, no. 6, p. 061 114, 2024. doi:10.1063/5.0213461

[20] P. Davis *et al.*, "Quantum efficiency measurements of a copper photocathode in an RF electron gun", in *Proc. PAC'93*, Washington, DC, USA, pp. 2976–2978, 1993. doi:10.1109/PAC.1993.309524

[21] S. Karkare and I. Bazarov, "Effects of surface nonuniformities on the mean transverse energy from photocathodes", *Phys. Rev. Appl.*, vol. 4, no. 2, p. 024 015, 2015. doi:10.1103/PhysRevApplied.4.024015

[22] Z. Huang *et al.*, "High responsivity and fast UV–vis–short-wavelength IR photodetector based on Cd_3As_2/MoS_2 heterojunction", *Nanotechnology*, vol. 31, p. 064 001, 2019. doi:10.1088/1361-6528/ab51d3

[23] D. H. Dowell and J. F. Schmerge, "Quantum efficiency and thermal emittance of metal photocathodes", *Phys. Rev. Spec. Top. Accel. Beams*, vol. 12, p. 074 201, 2009. doi:10.1103/PhysRevSTAB.12.074201

[24] P. Saha *et al.*, "Theory of photoemission from cathodes with disordered surfaces", *J. Appl. Phys.*, vol. 133, no. 5, p. 053 102, 2023. doi:10.1063/5.0135629

[25] C. M. Pierce, J. K. Bae, A. Galdi, L. Cultrera, I. Bazarov, and J. Maxson, "Beam brightness from Cs–Te near the photoemission threshold", *Appl. Phys. Lett.*, vol. 118, p. 124 101, 2021. doi:10.1063/5.0044917